

Satellite-Based Monitoring for Dam Infrastructure Safety and Risk Mitigation.

A Thesis submitted

In partial fulfilment of the requirement for the degree of

Master of Technology

Submitted By

MANISH BHAGAT

(234104617)

Under the supervision of Prof. Subashisa Dutta

(Professor)



DEPARTMENT OF CIVIL ENGINEERING

INDIAN INSTITUTE OF TECHNOLOGY GUWAHATI – 781039, Assam

November 2024

Indian Institute of Technology Guwahati



Department of Civil Engineering

STATEMENT

I, Manish Bhagat, do hereby declare that the matter embodied in this thesis and the results of investigations have been carried out by me under the supervision of Prof. Subhashisa Dutta at the Department of Civil Engineering, IIT Guwahati.

In keeping with the general practice of reporting scientific observations, due acknowledgements have been made wherever the work described and is based on the findings of other investigations.

Date: 28th November 2024

(Manish Bhagat)

Indian Institute of Technology Guwahati



Department of Civil Engineering

ACKNOWLEDGEMENT

With the completion of my thesis, I would like to express my deep feeling of appreciation to my thesis supervisor Prof. Subashisa Dutta for his guidance and constant support throughout my project work. I am thankful to him for clarifying my doubts and giving necessary insights for the topic.

I would also like to thank my seniors Dr Ketan Kumar Nandi, Manish Rana, Om Prakash Maurya, Saikat Das, for their continuous support, advice and invaluable feedback during my project.

I would also like to thank my classmates and my close friends Aalbin Simon, Sohel Ahmed for their unconditional friendship, support and patience throughout my project work.

Finally, I would like to thank my parents for their support and encouragement. I also place on record, my sense of gratitude to one and all who, directly or indirectly, have lent their helping hand in this journey.

Table of Contents

1. Chapter	1
1.1 Introduction.....	1
1.2 Objective of the Study	4
2. Chapter: Literature Review	5
2.1 General	5
2.2 SAR data used for Dam Structural Stability and Deformation Monitoring	5
2.3 SAR data used Monitoring Subsidence Landslide and Slope Stability Analysis in Reservoir Areas 7	
2.4 Need for Study.....	11
3. Chapter: Study Area and Dataset.....	12
3.1 Overview.....	12
3.2 DATASETS USED.....	14
3.3 ASF (Alaska Satellite Facility) Vertex:	14
3.4 Sentinel-1	14
4. Chapter: Methodology and Material.....	18
4.1 Overview.....	18
4.2 Data Acquisition	18
4.3 Software Used	21
4.3.1 InSAR Technology	23
4.4 Data Processing Algorithm	25
4.5 Pre-Processing.....	25
4.6 Post Processing.....	27
5. Chapter: Results and Discussion	30
5.1 Phase Difference	30
5.2 Displacement Map	31
6. Chapter	32
6.1 Future Scope.....	32
7. REFERENCES	33
.....	33

LIST OF FIGURES

Figure 1: Teesta River Basin (source: SANDRP web, 2018)	2
Figure 2: (a) Dam area and watershed area along the upstream river, (b) The deformation map of InSAR Sentinel-1 data (ascending and descending) from June 2022 to August 2023 at the study area. The red color indicates a ground movement > 6cm / year, while green shows stable behavior or no deformation observed.	5
Figure 3: The result of L-band radar data SAOCOM satellite at the study area using different time period.	6
Figure 4: Measured deformation(mm/yr) for QPSs. The threshold to select a QPS is 0.75 (source: Wang et al., 2011).....	7
Figure 5: The two dams under investigation (a, b) and A-DInSAR results (c). For every measurement point, it is possible to observe the displacement rate in mm/year. Negative values (yellow to red) are points with deformation rate away from the satellite, while positive values (light blue to dark blue) are points that move towards the sensor. Green points are stable. (COSMO-SkyMed Product - ©ASI - Agenzia Spaziale Italiana -(2017). All rights reserved).	8
Figure 6: Pleiades satellite images taken just before and after the tragedy, showing the water from Dam-VI, the tailings from Dam-I, and the Corrêgo do Feijão stream.....	9
Figure 7: Time-series of LoS displacement for two selected points located at the bottom of the dam showing the maximum cumulative displacements for the entire monitoring period and the accumulated pluviometric data.	9
Figure 8: Sentinel-1 PS-InSAR results, processed on SARscape Analytics with a minimum coherence of 0.65, for the 9 April 2019 Hindalco TSF failure in India. A Line-of-sight (LOS) velocity map, annotated with the data points selected for time-series analysis. Negative (red) values indicate detected movements away from the satellite, positive (blue) values indicate detected movements toward the satellite, and green-yellow values indicate detected stable areas. B Cross sectional schematics illustrating the geometric relationship between the satellite, the dam, and the PS points selected for time-series analysis. The small red arrows indicate the direction of detected LOS movement, in this case away from the satellite. C Cumulative LOS displacement time-series for the selected data points.	10
Figure 9: Location of Study Area, 1. India map Esri National Geographic, 2 Sikkim, in pink color boundary, 3. Sikkim with South Lhonak Lake.	12
Figure 10: Illustration of ascending and descending satellite orbits(source- uploaded by Renalt Capes.	15
Figure 11: Sentinel-1 Acquisitions Swath Coverage. [Credits: ESA]	16
Figure 12: Flow Diagram which show Microwave Remote Sensing system to Synthetic Aperture Radar.	18
Figure 13: side-looking geometry Forming a Radar Image, Vs/c -velocity of satellite or aircraft, source- Alaska Satellite Facility (ASF),Source- Early Adopter Workshop 2024.....	19
Figure 14: Alaska Satellite Facility (ASF) NASA-ISRO SAR Mission (NISAR).....	24
Figure 15: Visualization of the interferogram generation workflow	26
Figure 16: Alaska Satellite Facility (ASF) NASA-ISRO SAR Mission (NISAR).....	27
Figure 17: Processed Unwrapped Interferogram, (Projected on Google Earth Pro)	30
Figure 18: (1) Image generated from SNAP which showing displacement ranging from -0.0487 m to -0.01948 m in water shed area, (2) Teesta stage 3 Dam before event and after dam breach, source: SANDRP web, 2018.....	31

1. Chapter

1.1 Introduction

The Land deformations is concept used to describe changes in the Earth's surface, in the context of geology, geophysics, or remote sensing. It refers to any change in the shape or structure of the Earth's surface over time. It can involve uplift, subsidence, tilting, or bending of the ground. Deformation can occur on both large (e.g., tectonic plate movement) and small scales (e.g., localized subsidence due to mining and construction). It causes by Earthquakes (Sudden shifts along faults), Landslides (Movement of land masses), Volcanic activity (Movement of magma beneath the earth surface can lead uplift or subsidence, or lateral displacement) or Anthropogenic activities (Human activity that impacts the environment, either directly or indirectly). But most often affecting mountainous or hilly terrain, landslides occur when a large mass of dirt, rock, mud, and other materials are suddenly pulled downward by the force of gravity. These events can be disastrous for nearby communities, destroying property and infrastructure as well as resulting in loss of life.

Some Ground displacement events occurred over a world, by natural causes are the Kanto region, Japan, which has been affected by the 2011 Tohoku earthquake of magnitude 9.1 caused a massive Surface displacement of up to 5 meters horizontally and 1.2 meters vertically (ElGharbawi, T., et al 2015). Mount Etna, Italy is one of the most active volcanoes in the world, showing frequent episodes of inflation and deflation due to magma movement Tracked surface uplift of several centimeters per year caused by magma intrusion (Pezzo, G., et al 2023). Land Subsidence incident occurred in Mexico City; Mexico due to groundwater extraction has caused land subsidence Detected subsidence rates of up to 50 cm per year in some areas (Cigna, F., et al 2021).

Also, India has experienced several incidents of land deformation and displacement due to earthquakes, landslides, subsidence, and human activities. The Himalayan town of Joshimath, (2023) experienced significant subsidence due to construction, groundwater depletion, and natural causes. ISRO's National Remote Sensing Centre (NRSC) used satellite data to confirm ground subsidence of 5.4 cm over 12 days in December 2022–January 2023 (Sinha et al., 2024). Subsidence because of overextraction of groundwater has led to land subsidence in parts of Delhi and surrounding areas. Studies detected subsidence rates of up to 12 cm per year in areas like Gurugram (Malik et al., 2022). One more example of landslide occurred in Raigad, Maharashtra, India. The landslide was caused by torrential rains.

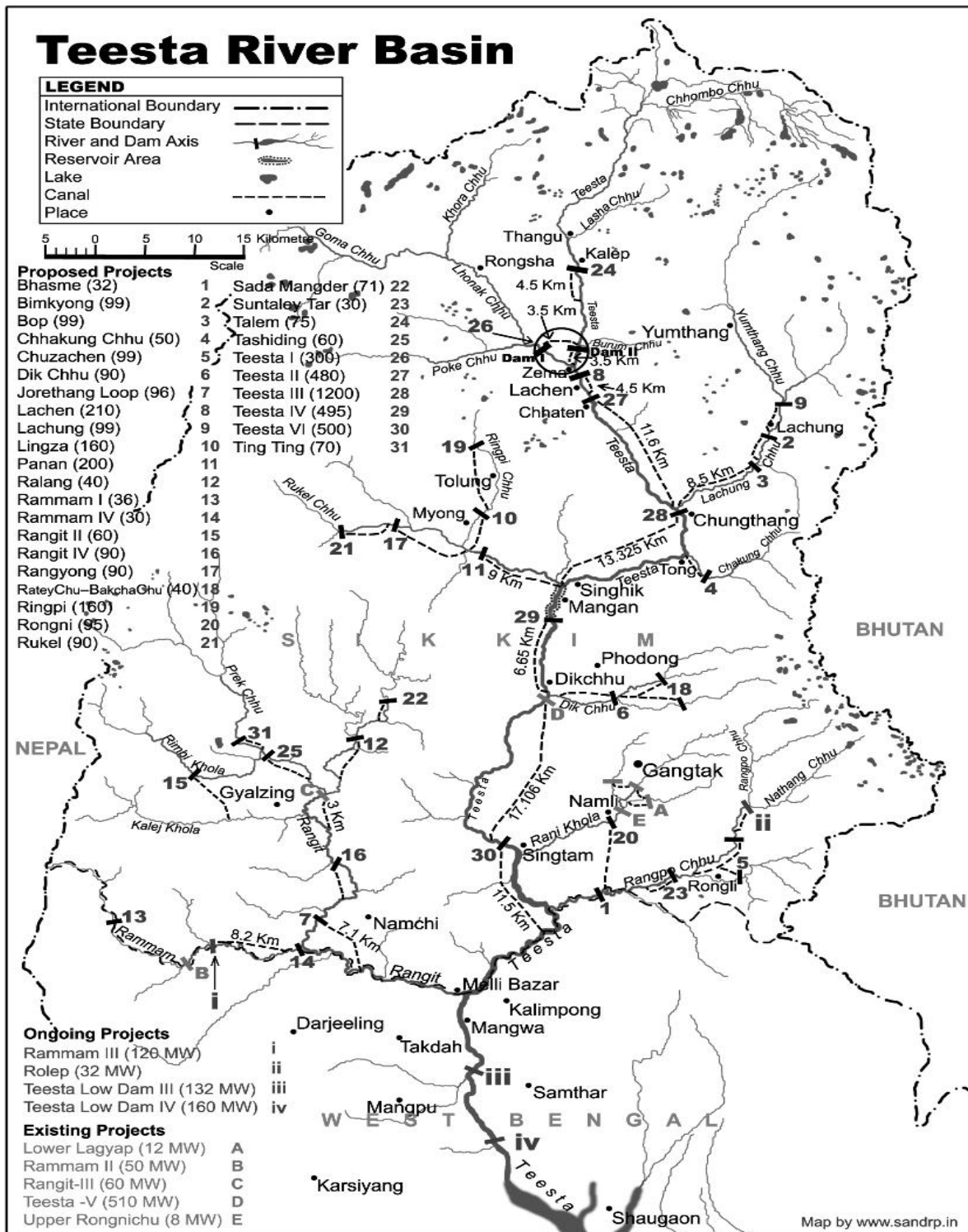


Figure 1: Teesta River Basin (source: SANDRP web, 2018)

Land deformation directly impacts the safety and functionality of Dam Infrastructure. Dams are massive structures that rely on the stability of their foundations and the surrounding environment. Deformation in the Earth's surface, whether it's caused by natural phenomena

earthquake and Fault Movement or human-induced forces, can compromise the integrity of dams, reservoirs, and related systems, potentially leading to catastrophic failures. Key links between ground deformation and dam safety ground uplift and subsidence can alter the pressure distribution at the dam base, leading to cracks or instability. Landslides and Slope Instability into reservoirs can displace large volumes of water, generating waves that may overtop or damage the dam. Slope deformation near dams increases the risk of landslides. Deformation in Surrounding Infrastructure Spillways, tunnels, and powerhouses connected to dams are highly sensitive to deformation. Subsidence or uplift can misalign these structures, reducing their efficiency or causing failures. Also, the magma movement under volcanic regions near dams can cause uplift and compromise the structure. Subsidence can weaken the dam foundation, distort spillways, or lead to the formation of cracks in the structure.

Recent dam failures in India, such as the 2023 breach of the Teesta stage 3 hydroelectric power project in Sikkim and the Karam Dam collapse in Madhya Pradesh (Parkash et al. 2023), as well as in 2019 Tiware Dam failure in Maharashtra, and many more dams failed they all highlight the urgency for effective dam safety measures. These events resulted in significant damage, land erosion, and loss of life. These all incident may be happened due to many Factors, including poor maintenance, design flaws, underscoring vulnerabilities, especially in regions landslide, Earthquake prone to extreme weather and climate change-induced stressors.

Interferometric Synthetic Aperture Radar (InSAR) technology has emerged as a powerful remote sensing tool that can detect surface deformation over large areas by comparing phase changes between satellite images captured at different times. This technology is used to Detection and Monitoring of Landslides Using he persistent scatterers InSAR (PSI) method in Gangtok, Sikkim Himalaya (Bhasin et al., 2023). Bui et al., 2021 has detected land deformation by Sentinel-1A InSAR data (2016–2020) over Hanoi, Vietnam. The results show that Dan Phuong/Hoai Duc and HaDong/Thanh Tri districts with the mean subsiding rates of ~5 mm per year. Wang et al., 2011 has carried out a combination of permanent scatterer and quasi permanent scatterer time-series InSAR image analyses to extract geometric information over the area of the Three Gorges Dam for detecting deformation.

Among the numerous InSAR deformation analysis techniques (Aswathi et al., 2022), Persistent Scatterer (PS) is able to produce highly precise, long-term displacement time series mainly for human-built structures such as bridges, roads, buildings, and dams (Ferretti et al., 2001; Crosetto et al., 2016). Small Baseline Subset (SBAS) InSAR is an alternative time-series

approach that was designed to improve the spatial distribution and density of “Distributed Scatterer” (DS) observation points in vegetated study areas, albeit at reduced spatial resolution (Berardino et al. 2002; Casu et al., 2006).

This paper explores the application of InSAR technology for long-term monitoring of dams, using a case study from the Teesta River in Sikkim. The analysis leverages Sentinel-1A satellite data to identify and evaluate deformation patterns, contributing to better risk management and proactive safety measures. The study emphasizes the importance of integrating modern monitoring tools to prevent future dam failures and enhance resilience in water infrastructure systems.

1.2 Objective of the Study

Following are the key objectives of the study:

- a) Assess Ground Deformation: Identify high-deformation hotspots, which is important for hazard assessment.
- b) Structural Integrity: Obtain how much displacement or deformation of the dam reservoir and itself.
- c) Processing methods for Interferometric Synthetic Aperture Radar (InSAR) and obtaining phase to displacement using SNAP.

2. Chapter: Literature Review

2.1 General

In these studies, have demonstrated the following key interactions between ground deformation and dam safety. Monitoring dam health has become a vital aspect of infrastructure management, with advancements in remote sensing technologies, particularly Interferometric Synthetic Aperture Radar (InSAR), Several case studies highlight the effectiveness of InSAR in land deformation and mitigating dam-related risks:

2.2 SAR data used for Dam Structural Stability and Deformation Monitoring

Dwitya et al 2024 In this study, the area of concern is divided into two main areas: The dam area and the watershed area along the upstream river, approximately 5 kilometres from the hydroelectric dam. The dataset used in this work consists of 392 images of Sentinel-1 from 1 September 2018 to 11 August 2023 to conduct long-term InSAR data analysis.

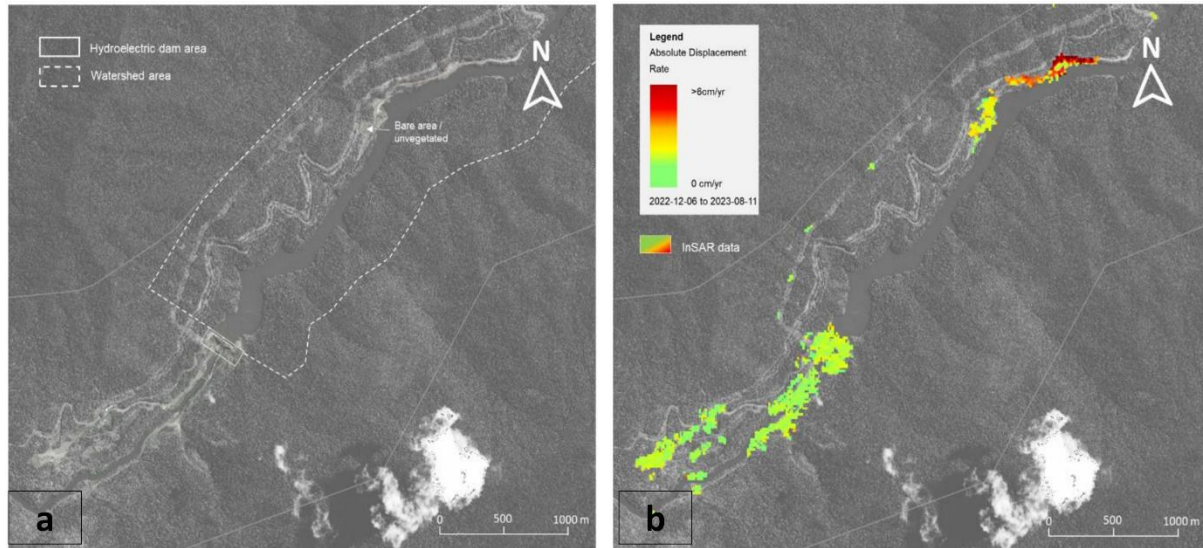


Figure 2: (a) Dam area and watershed area along the upstream river, (b) The deformation map of InSAR Sentinel-1 data (ascending and descending) from June 2022 to August 2023 at the study area. The red color indicates a ground movement $> 6\text{ cm / year}$, while green shows stable behavior or no deformation observed.

The result of InSAR data analysis presents the stable behavior of the dam during the period from 2018 – 2023. Horizontal trend in InSAR time series indicates no movement at the dam area, by checking pixel by pixel and group of pixels data. Based on the deformation analysis

of the watershed area using Sentinel-1, the linear deformation trends are detected with an average of deformation -4.7 cm from October 2022 to August 2023 as shown in figure. The upstream area is mostly covered by dense vegetation and the coverage of Sentinel-1 data is suboptimal, it has 456 pixels only over the bare/unvegetated area, around 1.2 kilometers from the total length of 5 kilometers watershed area or only 24% of the data, because C-band is using short wavelength and unable to penetrate through the vegetation. In this case, L-band radar with a longer wavelength can be used for monitoring watershed area because the capability to penetrate the vegetation.

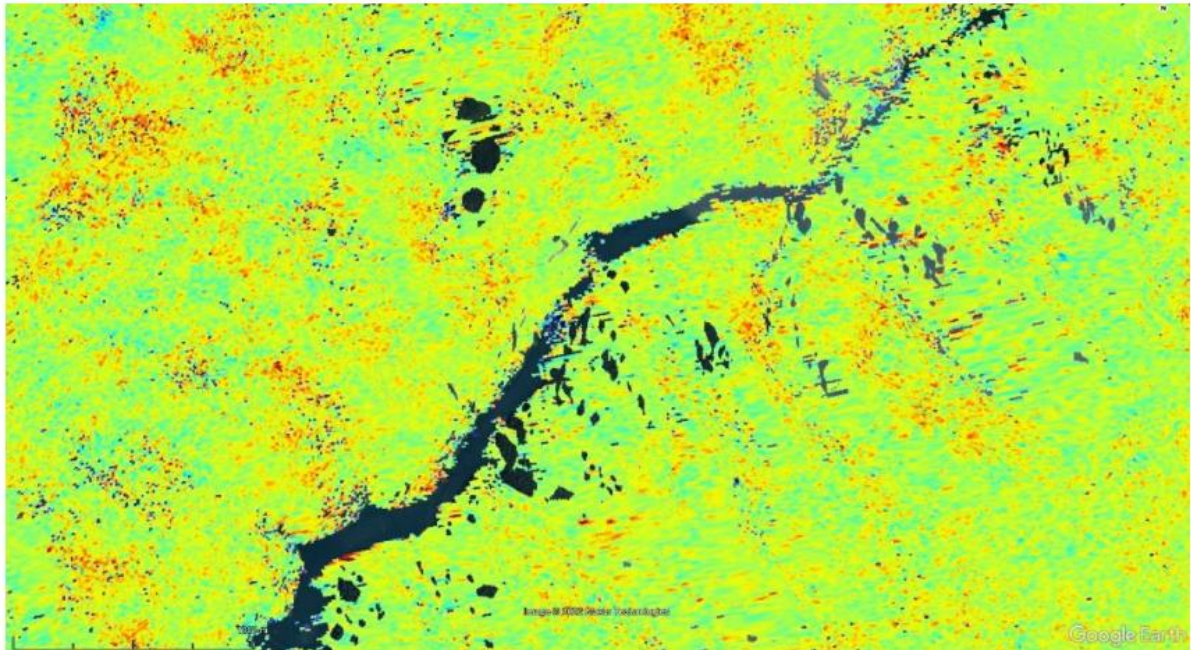


Figure 3: The result of L-band radar data SAOCOM satellite at the study area using different time period.

After field observation was conducted by the surveillance team on-site, the activity of scaling the slope along the moving area near road access was identified since 2022 there were no significant movement from September 2018 to November 2022. This confirms that the away movement/subsidence event captured by InSAR data is normal behavior and doesn't threaten to the dam safety.

Wang et al (2011) has analyzed the deformation of The Three Gorges Project (TGP), the largest hydroelectric project in the world, is one of the most significant constructed projects in China. The paper combines two advanced techniques-Permanent Scatterer (PS) and Quasi Permanent Scatterer (QPS) time-series InSAR image analyses. The authors successfully measured and analyzed the deformation of the Three Gorges Dam and its surrounding area using 40 SAR images collected from 2003 to 2008. The results indicate that the left part of the dam has ceased to deform, while the overall deformation is influenced by the changing levels of the Yangtze River. Additionally, seasonal deformation due to temperature variations was

observed. This insight is important for understanding how environmental factors affect dam stability.

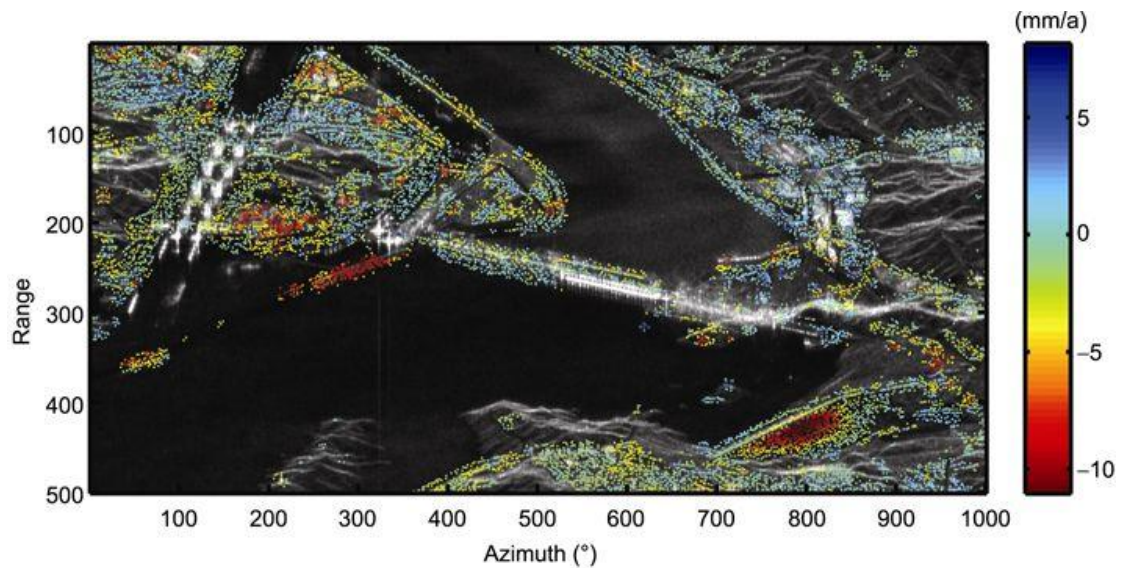


Figure 4: Measured deformation(mm/yr) for QPSs. The threshold to select a QPS is 0.75 (source: Wang et al., 2011)

The study also identified an area of abnormal subsidence near Zigui County, which could be critical for local infrastructure and safety assessments. This finding emphasizes the importance of continuous monitoring in regions with significant engineering structures like dams.

2.3 SAR data used Monitoring Subsidence Landslide and Slope Stability Analysis in Reservoir Areas

Antonielli et al 2018 conducted A preliminary site-specific PSI (Persistent Scatterer Interferometry) analysis has been carried out for two rock-fill dams in USA (Figure 5a, b). The two reservoirs serve as terminal basins for the water supply of Colorado Springs and surrounding municipalities. The A-DInSAR historical analysis has been performed using a stack of 114 high-resolution COSMO-SkyMed (form Italian Space Agency, ASI) scenes collected in the time span ranges between 2011 and 2016, in the ascending geometry of acquisition. The multi-image processing technique allowed the analysis of the past deformational behavior of the dam bodies. The velocity measurements have been obtained with millimeter accuracy in the LOS direction (the average velocity map is showed in Figure 5c). The measurement points in correspondence of the dam flanks show a general stability, while constrained ground deformations have been observed in the lower portion of the dam ‘b’ in

Figure 5c, where linear deformation behavior has been observed during the 5 years monitoring period, with an average velocity trend ranging between 3 and 7 mm/year.

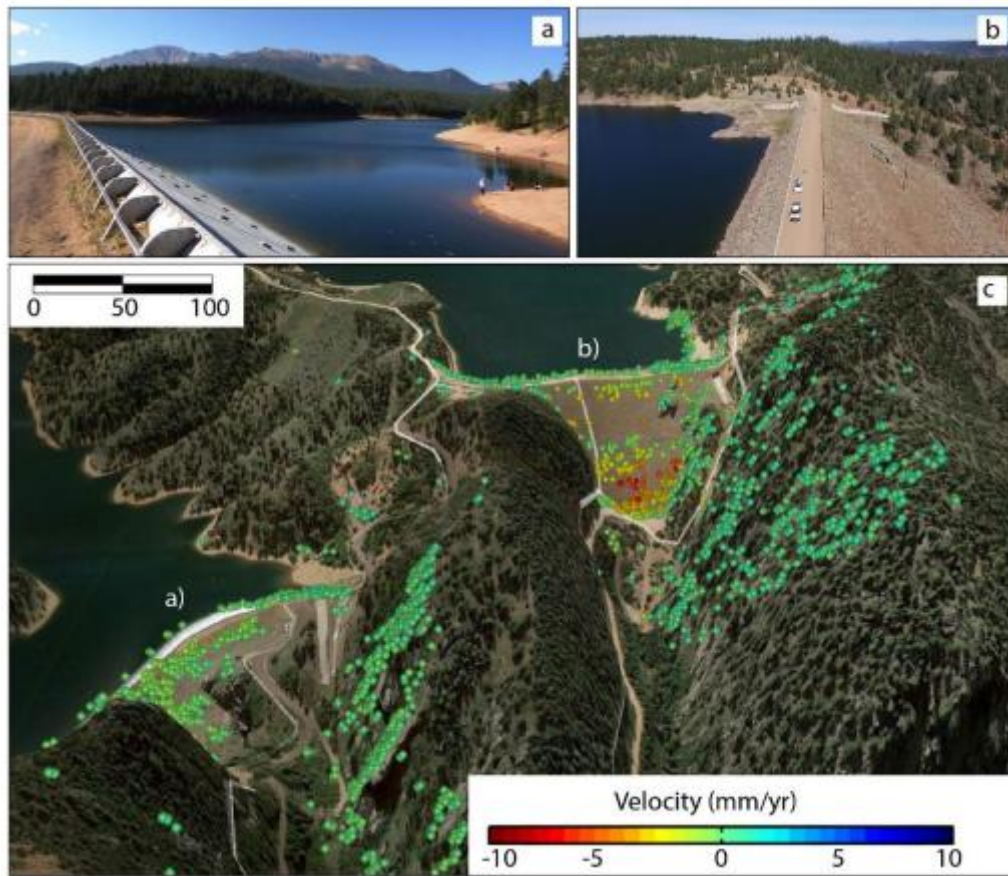


Figure 5: The two dams under investigation (a, b) and A-DInSAR results (c). For every measurement point, it is possible to observe the displacement rate in mm/year. Negative values (yellow to red) are points with deformation rate away from the satellite, while positive values (light blue to dark blue) are points that move towards the sensor. Green points are stable. (COSMO-SkyMed Product - ©ASI - Agenzia Spaziale Italiana -(2017). All rights reserved).

F. Gama 2020 In this research Differential Interferometric SAR (DInSAR) has been used to monitor surface deformations in open pit mines and tailings dams. In this paper, ground deformations have been detected on the area of tailings Dam-I at the Córrego do Feijão Mine (Brumadinho, Brazil) before its catastrophic failure occurred on 25 January 2019. Two techniques optimized for different scattering models, SBAS (Small Baseline Subset) and PSI (Persistent Scatterer Interferometry), were used to perform the analysis based on 26 Sentinel-1B images in Interferometric Wide Swath (IW) mode, which were acquired on descending orbits from 03 March 2018 to 22 January 2019. A WorldDEM Digital Surface Model (DSM) product was used to remove the topographic phase component. The results provided by both techniques showed a synoptic and informative view of the deformation process affecting the study area, with the detection of persistent trends of deformation on the crest, middle, and bottom sectors of the dam face until its collapse, as well as the settlements on the tailings.

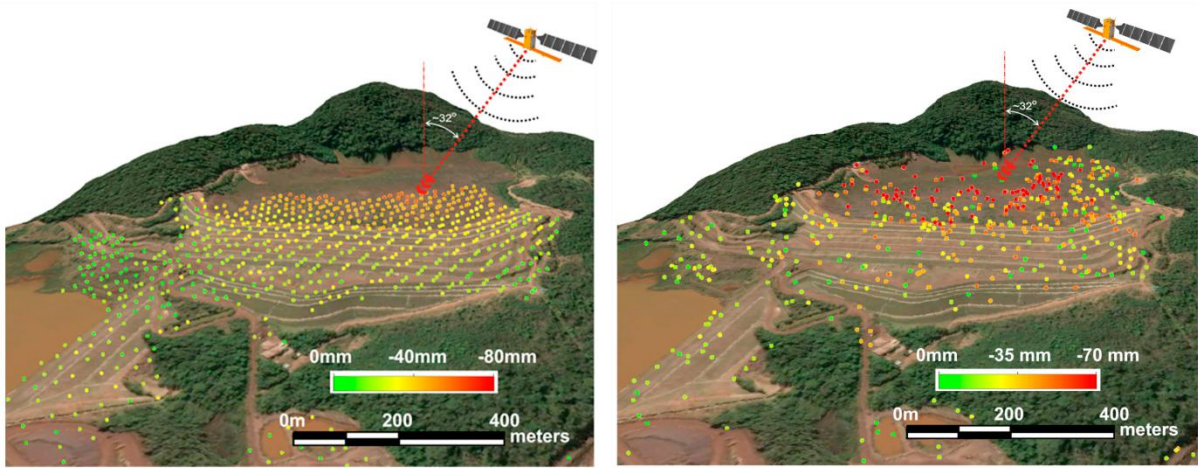


Figure 6: Pleiades satellite images taken just before and after the tragedy, showing the water from Dam-VI, the tailings from Dam-I, and the Corrêgo do Feijão stream.

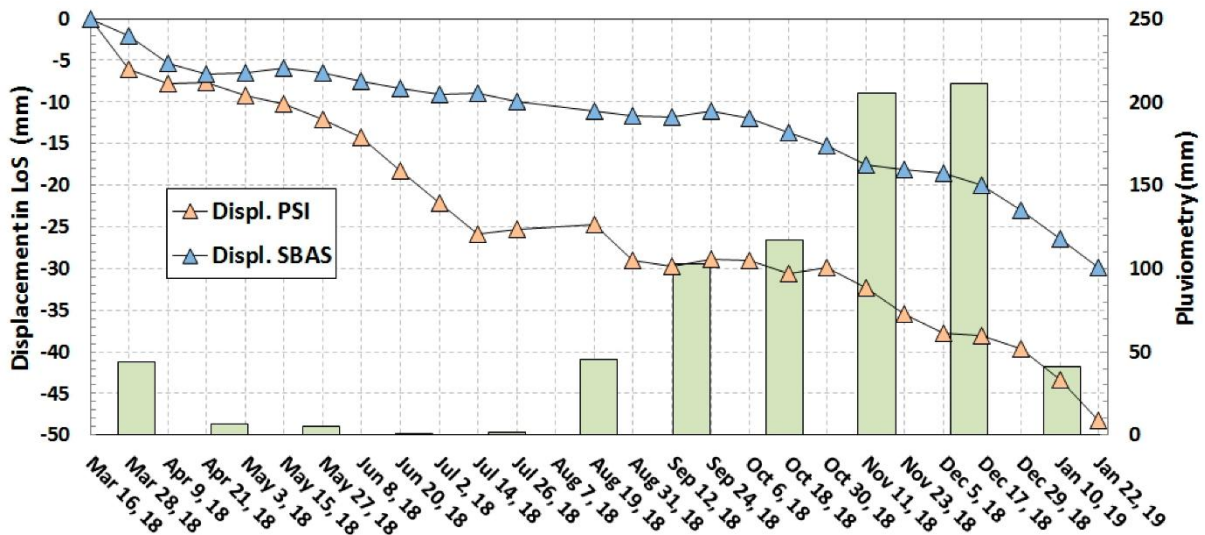


Figure 7: Time-series of LoS displacement for two selected points located at the bottom of the dam showing the maximum cumulative displacements for the entire monitoring period and the accumulated pluviometric data.

It is worth noting the detection of an acceleration in the displacement time-series for a short period near the failure. The maximum accumulated displacements detected along the downstream slope face were -39 mm (SBAS) and -48 mm (PSI). It is reasonable to consider that Sentinel-1 would provide decision makers with complementary motion information to the in-situ monitoring system for risk assessment and for a better understanding of the ongoing instability phenomena affecting the tailings dam.

Rana et al 2024 monitored and analyzed Tailings storage facilities (TSFs) impound mining waste behind dams to ensure public safety. This study investigates the failure of a bauxite residue tailings storage facility (TSF) operated by Hindalco Industries near Muri, Jharkhand, India, which occurred on 9 April 2019. The breached section involved about 600 meters of the southwest (SW) gabion retaining wall, impacting the area previously occupied by a water pond

and one of the storage ponds. This failure led to material flows constrained by nearby railway tracks and extending several hundred meters southward toward a village.

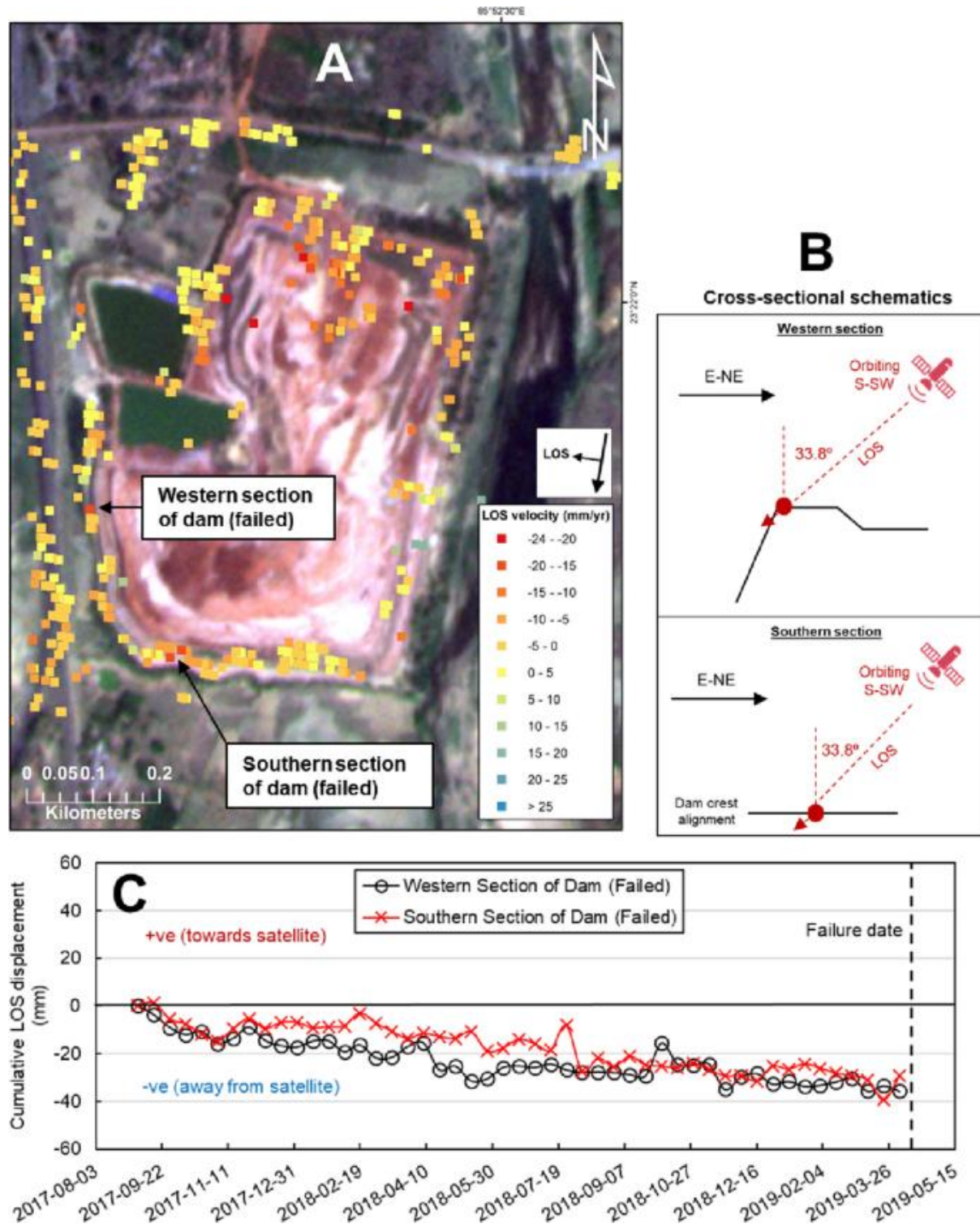


Figure 8: Sentinel-1 PS-InSAR results, processed on SARscape Analytics with a minimum coherence of 0.65, for the 9 April 2019 Hindalco TSF failure in India. A Line-of-sight (LOS) velocity map, annotated with the data points selected for time-series analysis. Negative (red) values indicate detected movements away from the satellite, positive (blue) values indicate detected movements toward the satellite, and green-yellow values indicate detected stable areas. B Cross sectional schematics illustrating the geometric relationship between the satellite,

the dam, and the PS points selected for time-series analysis. The small red arrows indicate the direction of detected LOS movement, in this case away from the satellite. C Cumulative LOS displacement time-series for the selected data points.

In summary, this paper contributes significantly to the understanding of dam stability through innovative methodologies, detailed measurements, and the identification of critical deformation patterns.

2.4 Need for Study

Using Sentinel-1 data, this study helps address this research gap in two ways. First, we present methods to process SAR data acquired by Sentinel-1 for displacement monitoring from open-source software such as SNAP (Sentinel Application Platform)/SNAPHU. Second, we examine the displacement in the region of Sikkim, West Bengal on Dams of Teesta River system. The traditional methods of dam monitoring, such as visual inspections, geotechnical sensors, and physical structural assessments, are effective but have limitations, especially when dealing with large-scale, remote, or difficult-to-access areas. InSAR technology offers a transformative approach to dam safety monitoring by enabling precise, wide-area, and non-invasive surveillance of dams and surrounding areas. Below are the key reasons for the increasing need and importance of InSAR technology in ensuring dam safety.

3. Chapter: Study Area and Dataset

3.1 Overview

The Teesta Stage III Hydropower Project, located in Chungthang, North Sikkim the dam coordinates: 27°35'52.04"N 88°39'1.13"E, is a key infrastructure project with a capacity of 1,200 MW. The project features a 60-meter-high concrete-faced rock-fill dam designed to harness the hydropower potential of the Teesta River.

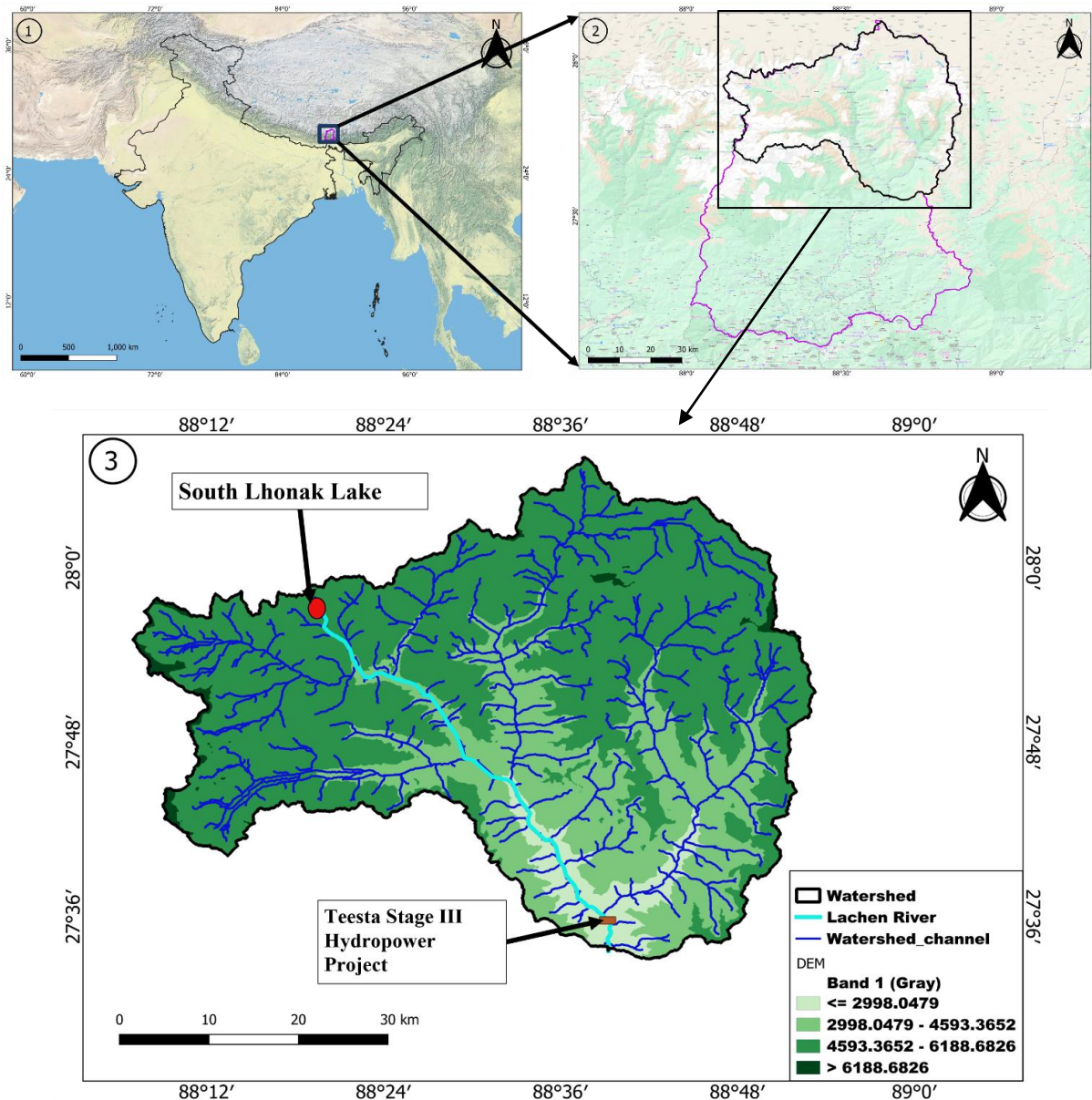


Figure 9: Location of Study Area, 1. India map Esri National Geographic, 2 Sikkim, in pink color boundary, 3. Sikkim with South Lhonak Lake.

Incident Context and Contributing Factors

The flood has brought unprecedented disaster all along the river in Sikkim and further downstream in West Bengal and then Bangladesh. Central Water Commission (CWC) reported early in the morning of Oct 4 that there was cloud burst at the site of the lake burst, the cloud burst could have played the role in triggering the lake burst. The Glacial Lake Outburst Flood (GLOF) was triggered by the sudden release of water from the glacier-fed South Lhonak Lake. The lake coordinates: 27°56'50.93"N 88°19'53.54"E. While initial theories suggested a cloudburst, rainfall data from the India Meteorological Department indicates that heavy rainfall occurred primarily in East and South Sikkim, not in the North Sikkim (Mangan) district, casting doubt on this hypothesis. The dam breach was exacerbated by its own water load of approximately five million cubic meters, which overwhelmed the spillway tunnels.

Design Limitations and Challenges

The spillway system of the Teesta Stage III project was designed to handle a maximum flood discharge of 7,000 cubic meters per second, accounting for rainfall-induced flooding but not GLOFs. Experts, including Himanshu Thakkar of the South Asia Network on Dams, Rivers, and People (SANDRP), have pointed out that this conservative design did not accommodate the unique and unpredictable dynamics of glacial lake outburst events, leaving the project vulnerable to such extreme scenarios.

Human and Economic Impact

The disaster has resulted in significant human and economic losses. Official estimates from the Sikkim State Disaster Management Authority report 42 fatalities as of November 1, 2023, with 77 people missing. Media reports suggest the toll could be as high as 82. The state-run National Hydroelectric Power Corporation Limited (NHPC) estimates the financial loss at approximately ₹233.56 crore (\$28 million).

Importance for Research

This incident highlights the complex interplay between hydropower infrastructure, glacial dynamics, and climate-induced risks. It underscores the need for comprehensive risk assessments and robust design considerations in glacial-fed river systems. The case study provides critical insights into disaster preparedness, infrastructure resilience, and sustainable hydropower development, making it a significant topic for academic research and policy formulation.

3.2 DATASETS USED

3.3 ASF (Alaska Satellite Facility) Vertex:

- **ASF Vertex** is likely referencing a term from the **Alaska Satellite Facility (ASF)**, which operates a data portal for accessing satellite imagery, including SAR datasets.
- The **Vertex** platform is ASF's web-based interface for discovering, searching, and downloading SAR data products from missions like Sentinel-1, ALOS PALSAR, and others.
- **Vertex** allows users to:
 - Visualize SAR acquisition footprints.
 - Search SAR data by geographic area, time, and other metadata..
 - Download RAW, SLC, and processed SAR products.

3.4 Sentinel-1

Sentinel-1 is a part of the European Space Agency's (ESA) Copernicus Programme, designed to provide Earth observation data for environmental monitoring, disaster management, and scientific research. Sentinel-1 consists of a pair of satellites, Sentinel-1A and Sentinel-1B (though Sentinel-1B ceased operation in December 2021), equipped with Synthetic Aperture Radar (SAR) to capture high-resolution radar images regardless of weather conditions or light availability.

Key Features of Sentinel-1

1. Synthetic Aperture Radar (SAR)

- **C-Band Radar:** Operates at a wavelength of approximately 5.6 cm, suitable for detecting surface changes.
- **All-Weather Capability:** SAR can penetrate clouds, rain, and darkness, enabling consistent monitoring.
- **Interferometric Capabilities:** Supports InSAR (Interferometric Synthetic Aperture Radar) to measure ground displacement and deformation with high precision.

2. Wide Swath Coverage

- Covers swaths up to 250 km with resolutions ranging from 5 m to 40 m, depending on the observation mode.
- Offers global coverage for both land and ocean monitoring.

3. Revisit Time

- Provides a revisit time of 6–12 days, which can be reduced further when using data from other SAR satellites (e.g., Sentinel-1A paired with Sentinel-1B previously).
- Ensures frequent monitoring of the same location for time-series analysis and deformation studies.

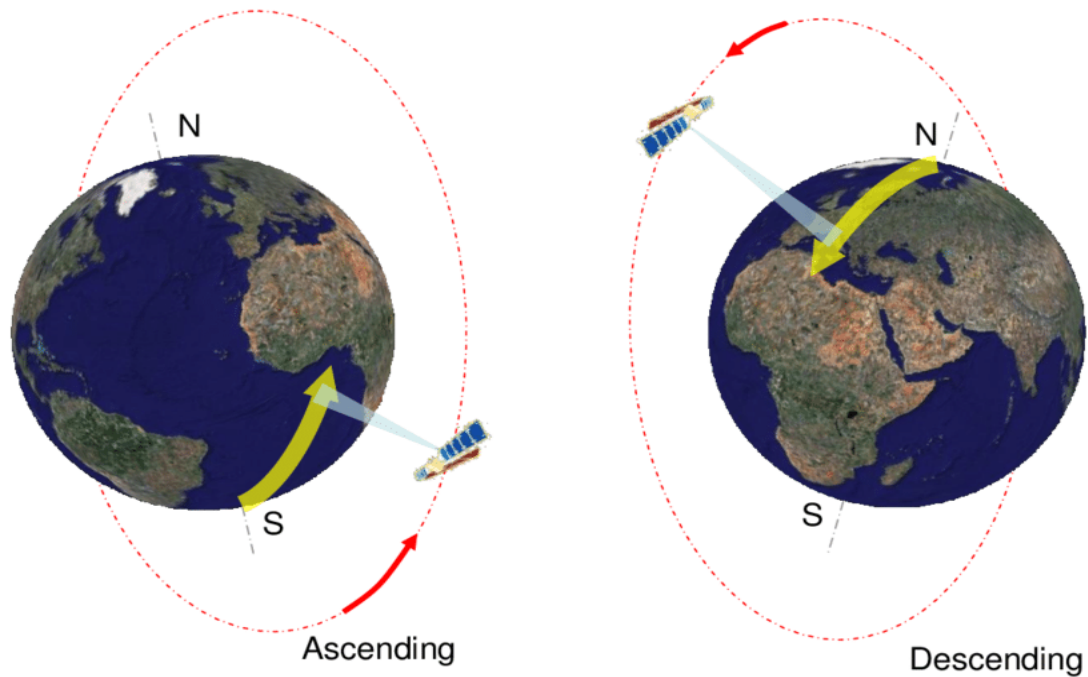


Figure 10: Illustration of ascending and descending satellite orbits(source- uploaded by Renalt Capes.

4. Data Accessibility

- Free and Open Data: Sentinel-1 data is freely available through platforms like Copernicus Open Access Hub and Alaska Satellite Facility (ASF), making it accessible to researchers worldwide.

Observation Modes

Sentinel-1 operates in four main imaging modes, each tailored for specific applications:

1. Interferometric Wide Swath Mode (IW):
 - Default mode for land monitoring.
 - Covers a wide area with high resolution, suitable for InSAR applications.

2. Stripmap Mode (SM):

- High-resolution imaging over smaller areas.
- Useful for localized studies requiring detailed imagery.

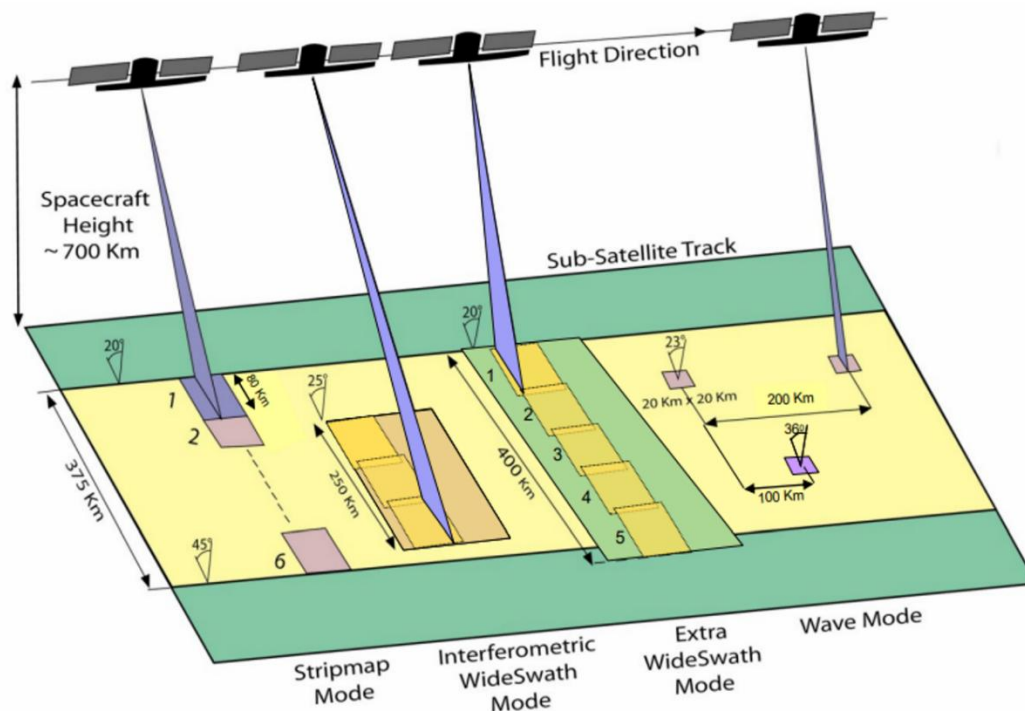


Figure 11: Sentinel-1 Acquisitions Swath Coverage. [Credits: ESA]

3. Extra-Wide Swath Mode (EW):

- Covers extremely large areas with medium resolution.
- Often used for maritime and coastal monitoring.

4. Wave Mode (WV):

- Special mode for ocean wave studies.
- Captures small, focused images of the sea surface.

Sentinel-1 Product

- Level-0 Products- Level-0 products are not currently disseminated to the community.
- Level-1 Products- Level-1 products can be one of two product types: either **Single Look Complex** (SLC) Ground Range Detected (GRD).
- Level-1 Products- Level-2 consists of geolocated geophysical products derived from Level-1.

In this project Interferometric Wide Swath Mode acquisition, Level-1 SLC product of acquires data with a 250km swath at 5m x 20m spatial resolution (single look) has been used.

4. Chapter: Methodology and Material

4.1 Overview

A **Microwave Remote Sensing System** uses microwave radiation (typically with wavelengths ranging from millimeters to meters) to observe and analyze Earth's surface. In **Interferometric Synthetic Aperture Radar (InSAR)**, a specialized form of microwave remote sensing, the system utilizes the phase differences of radar signals captured from multiple acquisitions to measure surface properties like topography and surface deformation.

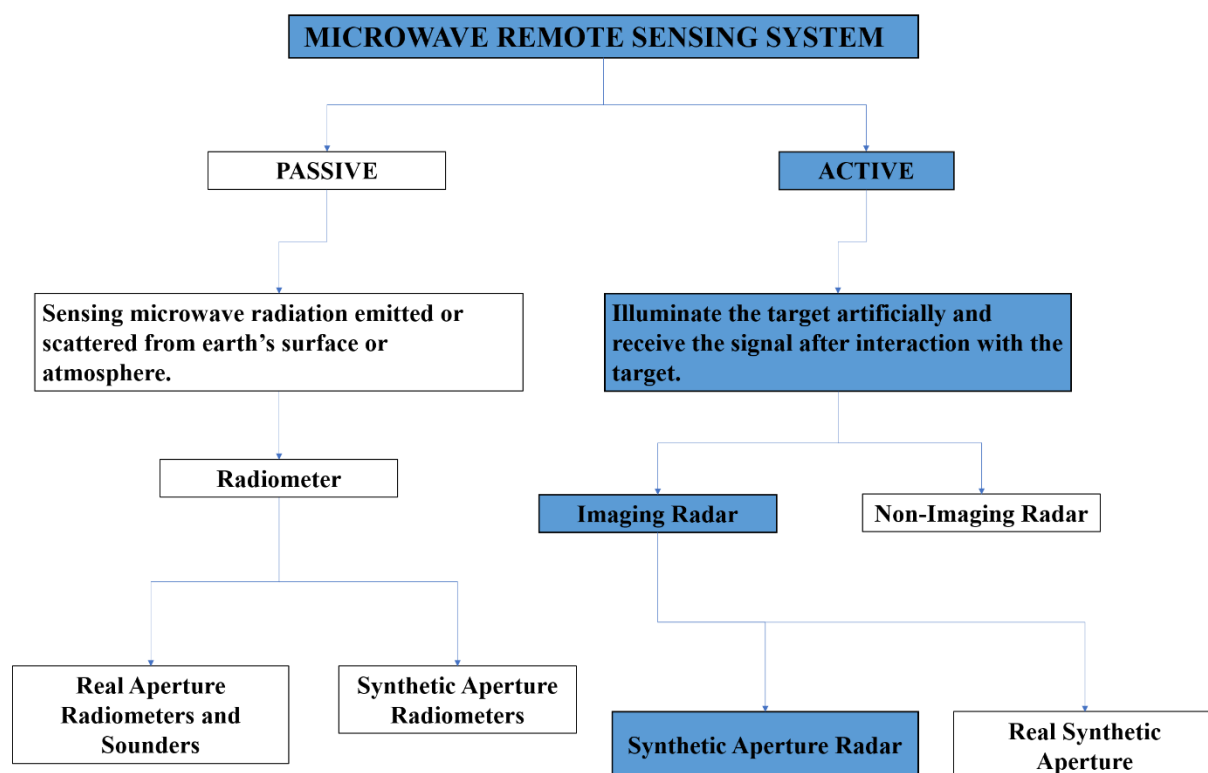


Figure 12: Flow Diagram which show Microwave Remote Sensing system to Synthetic Aperture Radar.

4.2 Data Acquisition

Side Looking Radar

Satellite use vertically downward-looking radar by which illuminates a circular patch. All the points on the periphery of the circular patch are at the same distance from the radar and hence the backscattered signals from the periphery reach the radar at the same time. This poses uncertainty in resolving from where the signal has arrived. This 'right-left' ambiguity can be

overcome if the radar illuminates to one side of the nadir off the platform (Satellite or spacecraft). Thus, imaging radar data is collected looking off to the side of aircraft or spacecraft. For remote sensing, side-looking imaging radars can be broadly classified into two categories:

- I. Real aperture radar usually referred to as SLAR (Side-Looking Airborne Radar) or SLR (Side-Looking Radar),
- II. Synthetic Aperture Radar (Modern SAR Sensors provide regularly sampled, high-resolution & weather-independent earth observation data from Space)

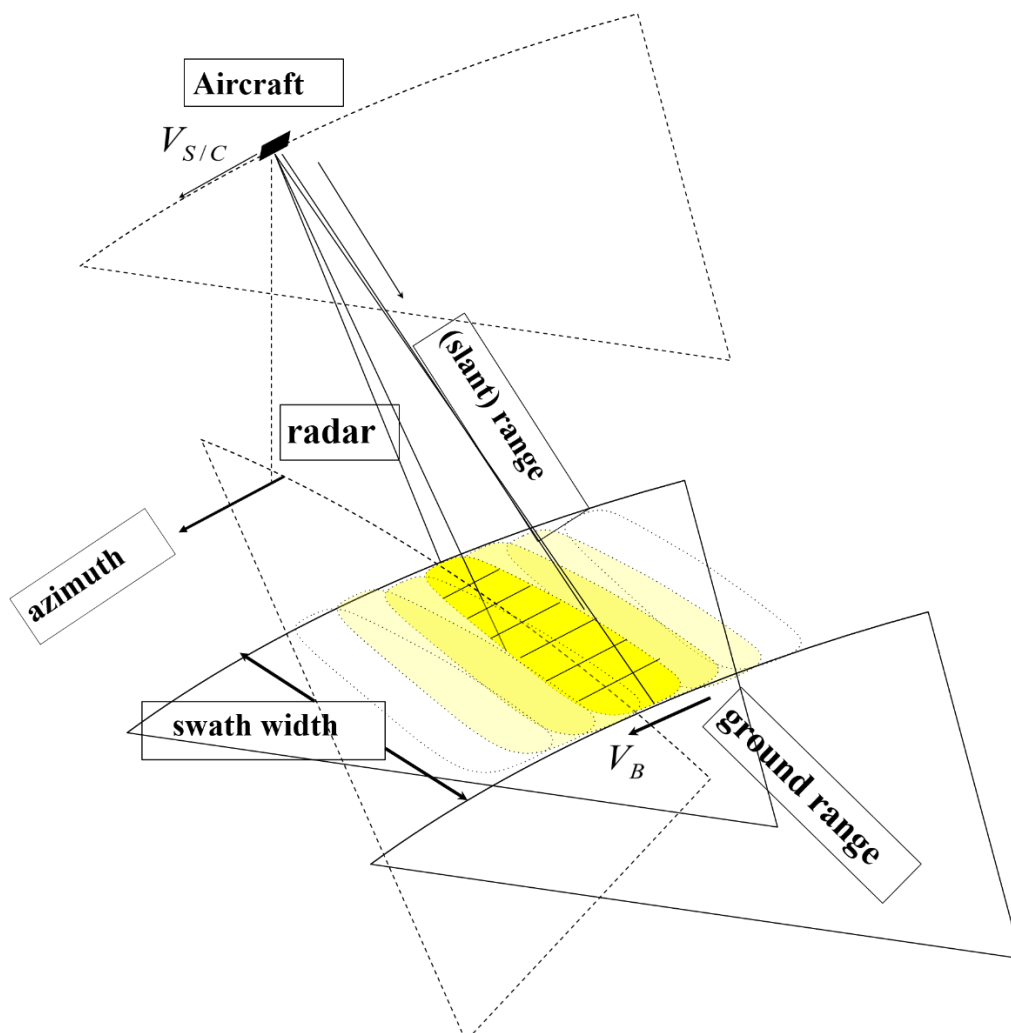


Figure 13: side-looking geometry Forming a Radar Image, $V_{s/c}$ -velocity of satellite or aircraft, source- Alaska Satellite Facility (ASF),Source- Early Adopter Workshop 2024.

SAR (Synthetic Aperture Radar) is an advanced remote active sensor technique that first transmits microwave signals and then receives back the signals that are returned, or backscattered, from the Earth's surface. that uses radar signals from satellites or aircraft to measure ground deformation with high precision. The methods provide a cost-effective, accurate method for tracking ground deformation, structural displacement, and surrounding environmental changes. The following methodology outlines the use of SAR for monitoring dam safety, emphasizing how it integrates with structural health monitoring systems. To mitigate these risks, advanced monitoring technologies are essential for monitoring and identifying potential risks and mitigating disasters such as dam breaches, structural deformation, or subsidence.

Table 1: Spectral Band with wavelength

Band	Frequency	Wavelength	Typical Application
P	0.3–1 GHz	100–30 cm	Biomass, vegetation mapping, and assessment. Experimental SAR band.
L	1–2 GHz	30–15 cm	Medium resolution SAR (geophysical monitoring, biomass and vegetation mapping, high penetration, interferometric SAR [InSAR])
S	2–4 GHz	15–7.5 cm	Increasing use for SAR-based Earth observation and agriculture monitoring (NISAR will carry an S-band channel; expends C-band applications to higher vegetation density)
C	4–8 GHz	7.5–3.8 cm	SAR Workhorse (global mapping, change detection, monitoring of areas with low to moderate penetration, higher coherence); ice, ocean, maritime navigation
X	8–12 GHz	3.8–2.4 cm	High resolution SAR (urban monitoring; ice and snow, little penetration into vegetation cover; fast coherence decay in vegetated areas)

The spatial resolution of radar data is directly related to the ratio of the sensor wavelength to the length of the sensor's antenna. For a given wavelength, the longer the antenna, the higher

the spatial resolution. From a satellite in space operating at a wavelength of about 5 cm (C-band radar), in order to get a spatial resolution of 10 m, you would need a radar antenna about 4,250 m long. (That's over 47 football fields). An antenna of that size is not practical for a satellite sensor in space. Hence, scientists and engineers came up with a clever workaround the synthetic aperture. In this concept, a sequence of acquisitions from a shorter antenna are combined to simulate a much larger antenna, thus providing higher resolution data.

4.3 Software Used

Software	Developer	Analysis Type	Applicable Platforms
1. Sentinel Application Platform (SNAP) Sentinel-1 Toolbox (S1TBX)	ESA (European Space Agency)	A graphical user interface (GUI) used for both polarimetric and interferometric processing of SAR data. Start to finish processing includes algorithms for calibration, speckle filtering, coregistration, orthorectification, mosaicking, and data conversion.	<ul style="list-style-type: none"> • Sentinel-1 • ERS-1 and 2 • ENVISAT • ALOS PALSAR • TerraSAR-X • COSMO-SkyMed
2. Statistical-Cost, Network-Flow Algorithm for Phase Unwrapping (SNAPHU)	Stanford Radar Interferometry Research Group	Software written in C that runs on most Unix/Linux platforms. Used for phase unwrapping (an interferometric process). The SNAPHU algorithm has been incorporated into other SAR processing software, including ISCE.	Input data is interferogram formatted as a raster, with single-precision.

Sentinel Application Platform (SNAP)

SNAP stands for Sentinel Application Platform, a software developed by the European Space Agency (ESA) to process and analyze satellite data, particularly from the Sentinel missions. It is a free, open-source, and cross-platform toolbox designed for remote sensing and Earth observation applications.

Key Features of SNAP

1. **Multisensor Support:**
 - Works with Sentinel-1 (SAR), Sentinel-2 (optical), Sentinel-3 (ocean and land data), and many other Earth observation missions.
2. **Graphical User Interface (GUI) and Command Line:**
 - Provides an easy-to-use interface and a command-line processor for automation.
3. **Data Processing:**
 - Supports preprocessing steps such as calibration, co-registration, geocoding, and atmospheric correction.
 - Can perform advanced operations like interferometric SAR (InSAR), polarimetric SAR (PolSAR), and optical image classification.
4. **Interoperability:**
 - Compatible with multiple formats such as GeoTIFF, NetCDF, and more.
 - Integrates with other tools like Python, R, and GIS software.
5. **Graph Processing Framework (GPF):**
 - Allows users to build workflows visually or programmatically to automate processing chains.
6. **Toolboxes for Specific Sensors:**
 - Includes toolboxes specifically tailored for SAR, optical, and atmospheric data processing.
7. **Visualization:**
 - Provides tools for visualizing and analyzing data, including band arithmetic, color manipulation, and 3D terrain views.

Applications of SNAP

- Interferometric SAR (InSAR): For measuring surface deformations, subsidence, or earthquakes.
- Land Use and Land Cover Analysis: Using optical data for classification and change detection.
- Oceanography: Analyzing ocean parameters like sea surface temperature and chlorophyll concentration.
- Climate Monitoring: Studying environmental and atmospheric changes over time.

It's widely used in research, academia, and operational monitoring systems for Earth observation.

4.3.1 InSAR Technology

- Synthetic aperture radar (SAR) satellites actively emit microwave radiation towards the Earth's surface and measure the portion of it that returns.
- By comparing synthetic aperture radar measurements from two different dates, InSAR produces a measurement of the change in the ground position between the two dates.
- By comparing observations from many dates, the movement pattern of a dam or reservoir rim over time can be obtained.
- InSAR measures phase difference between two SAR acquisitions.
- The interferometric phase, between two SAR images acquired at different times over the same region from the similar viewing geometry, can represent ground movements.
- The phase difference is equivalent to range change or distance change between radar and target.

Mathematical formulation of InSAR phase components

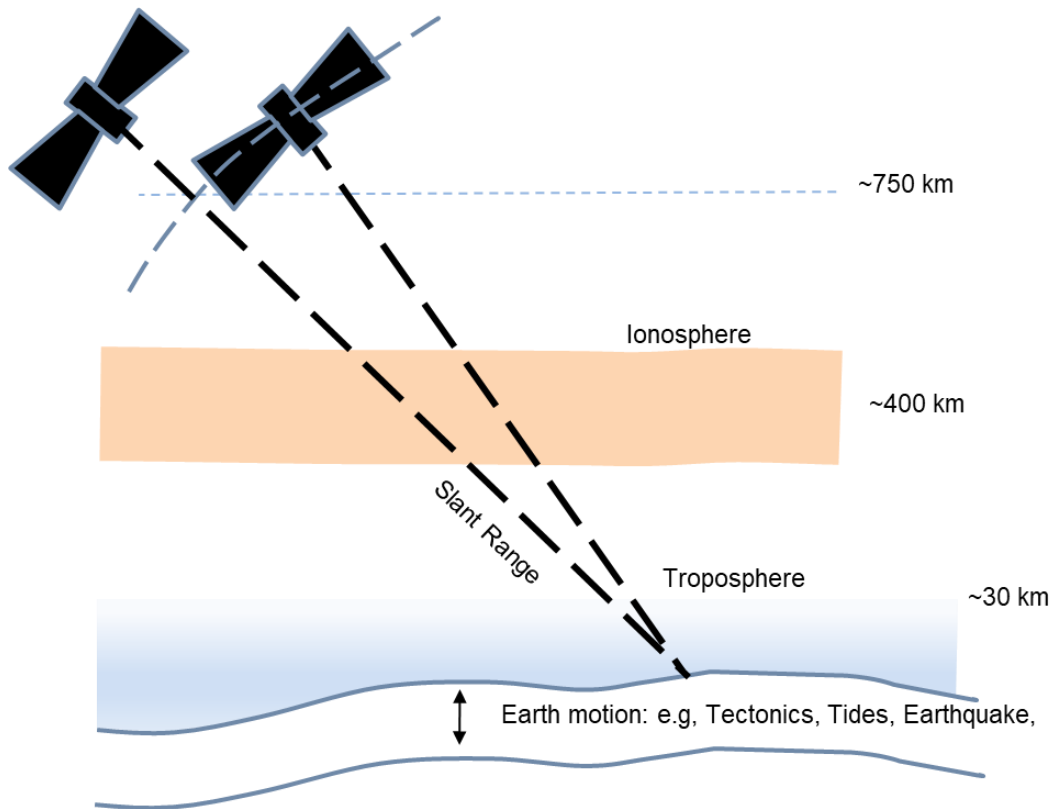


Figure 14: Alaska Satellite Facility (ASF) _NASA-ISRO SAR Mission (NISAR)

Source- Early Adopter Workshop 2024.

$$\delta\phi = \delta\phi_{displacement} + \delta\phi_{atmosphere} + \delta\phi_{geometry} + \delta\phi_{scattering} + \delta\phi_{nois}$$

ϕ is Phase Difference

$\delta\phi$	Tota Phase Differenc
$\delta\phi_{displacement}$	Surface displacement
$\delta\phi_{atmosphere}$	Atmospheric delay
$\delta\phi_{geometry}$	Introduced by non-zero baseline
$\delta\phi_{scattering}$	Surface scattering components

4.4 Data Processing Algorithm

4.5 Pre-Processing

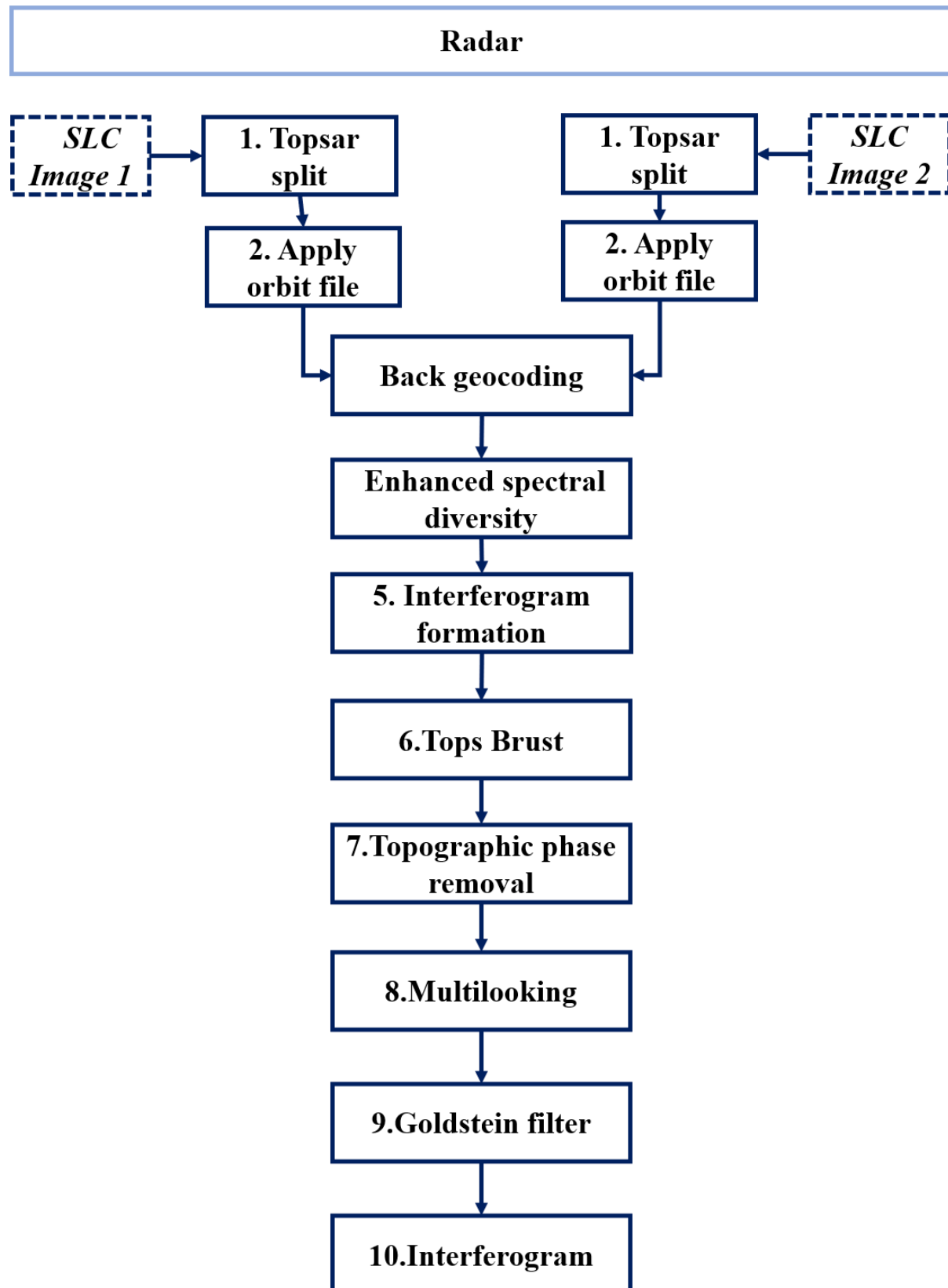


Figure 15: Visualization of the interferogram generation workflow

Prerequisites Materials List

1.Sentinel-1 Toolbox SNAP

2. Data (sample images provided). Accessed from ASF's Vertex.

Pre-event sample SLC:

- S1A_IW_SLC__1SDV_20230925T121408_20230925T121435_050484_061484_C0C9

- Post-event sample SLC:

- S1A_IW_SLC__1SDV_20231007T121408_20231007T121435_050659_061A83_4B1E

Single Look Complex (SLC): SLC is a type of radar image format commonly used in Synthetic Aperture Radar (SAR) systems. It is a high-resolution, raw data product that preserves the phase and amplitude information of the radar signals, making it essential for applications such as interferometry (InSAR).

Processing RAW SLC (Single Look Complex) images in SNAP (Sentinel Application Platform) is essential for obtaining an **interferogram** and analyzing **land deformation** for several reasons. RAW SLC images contain unprocessed or minimally processed SAR data in its most detailed form, which needs to undergo systematic steps to extract meaningful information about surface changes.

Interferometry:

In an interferogram, fringes represent the phase differences between two radar signals captured by Synthetic Aperture Radar (SAR) sensors at slightly different positions or times. These phase differences are mapped into a color-coded or grayscale pattern of fringes, providing insights into topography, surface deformation, or other changes.

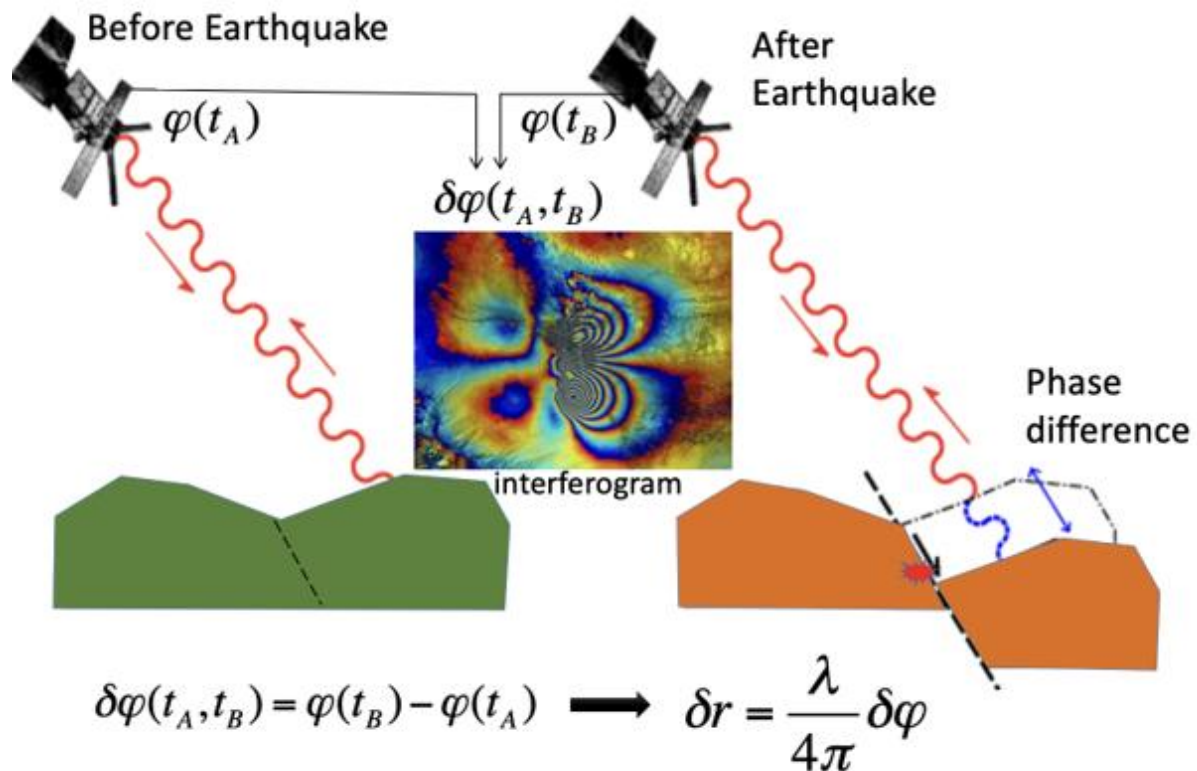


Figure 16: Alaska Satellite Facility (ASF) NASA-ISRO SAR Mission (NISAR)

Early Adopter Workshop_ January 2024.

4.6 Post Processing

In this includes unwarp the generated interferogram from pre processing and after that convert that unwrapped phase to displacement

The latest version of Sentinel-1 Toolbox (S1TBX) called SNAP is used for further process.

Step-1. Unwrap the Interferogram

a) Snaphu Export

Radar > Interferometric > Unwrapping > Snaphu Export

b) Snaphu Unwrapping in a Linux command line

c) Snaphu Import

Radar > Interferometric > Unwrapping > Snaphu Import

Step-2. Creating a Deformation Map

This step converts the unwrapped differential phase value (radians) to a displacement value (in meters) along the line of sight of the sensor.

This is computed using the following equation:

$$d = -\frac{\lambda}{4\pi} \Delta\varphi_d$$

Where λ is Sentinel-1's C-band SAR wavelength 5.6cm and $\Delta\varphi_d$ is the unwrapped phase difference between the two SLC images.

Step 3: Range-Doppler Terrain Correction

The Range-Doppler Terrain Correction operator applies a series of processes to the displacement map. First, it uses a Digital Elevation Model (DEM) to mask out areas without any elevation, including the ocean. This is helpful because none of the phase or displacement data over the ocean is useful. Second, it uses the DEM and a map projection system to orthorectify the image, projecting it onto the Earth's surface in its proper orientation. This operator also geometrically corrects SAR data, but this is not as relevant to this procedure as we only care about the included displacement and coherence bands which no longer include terrain geometry.

Step 4: Export as GeoTIFF

A GeoTIFF is a geospatial data file format that embeds geographic metadata into a standard Tagged Image File Format (TIFF). It allows the storage of spatial reference information, such as coordinate systems, map projections, and georeferencing, alongside raster image data. This makes GeoTIFF files ideal for use in Geographic Information Systems (GIS) and remote sensing applications.

Key Features of GeoTIFF

1. Embedded Georeferencing:

- GeoTIFF stores geospatial metadata directly in the file, including:
- Coordinate reference systems (CRS).
- Map projection details.
- Geotransform (origin, resolution, and rotation).

2. Raster Data Storage:

- It can store multi-band or single-band raster data, often used for:
- Satellite imagery.
- Digital Elevation Models (DEMs).
- Land cover maps.

Step 5: Consideration

Uplift or Subsidence?

The sign on our displacement maps can at sometimes be ambiguous. Interpreting the direction of displacement must be done carefully with respect to the master and slave combination of your two SLCs, as well as the expression used when converting the unwrapped phase interferogram to displacement. Recall that the Sentinel-1 Toolbox uses the following formula where λ is Sentinel-1's C-Band SAR wavelength and $\Delta\Phi_d$ is the unwrapped phase difference between the two SLCs.

$$d = -\frac{\lambda}{4\pi} \Delta\varphi_d$$

Our interferogram was created in the frame of reference of the satellite, meaning that the unwrapped phase values correspond to how much the distance between the surface and the satellite has changed. An increasing phase value indicates that this distance is increasing and what this actually corresponds to on the ground is subsidence. In this way, a positive unwrapped phase value will correspond with a negative displacement on the ground.

5. Chapter: Results and Discussion

5.1 Phase Difference

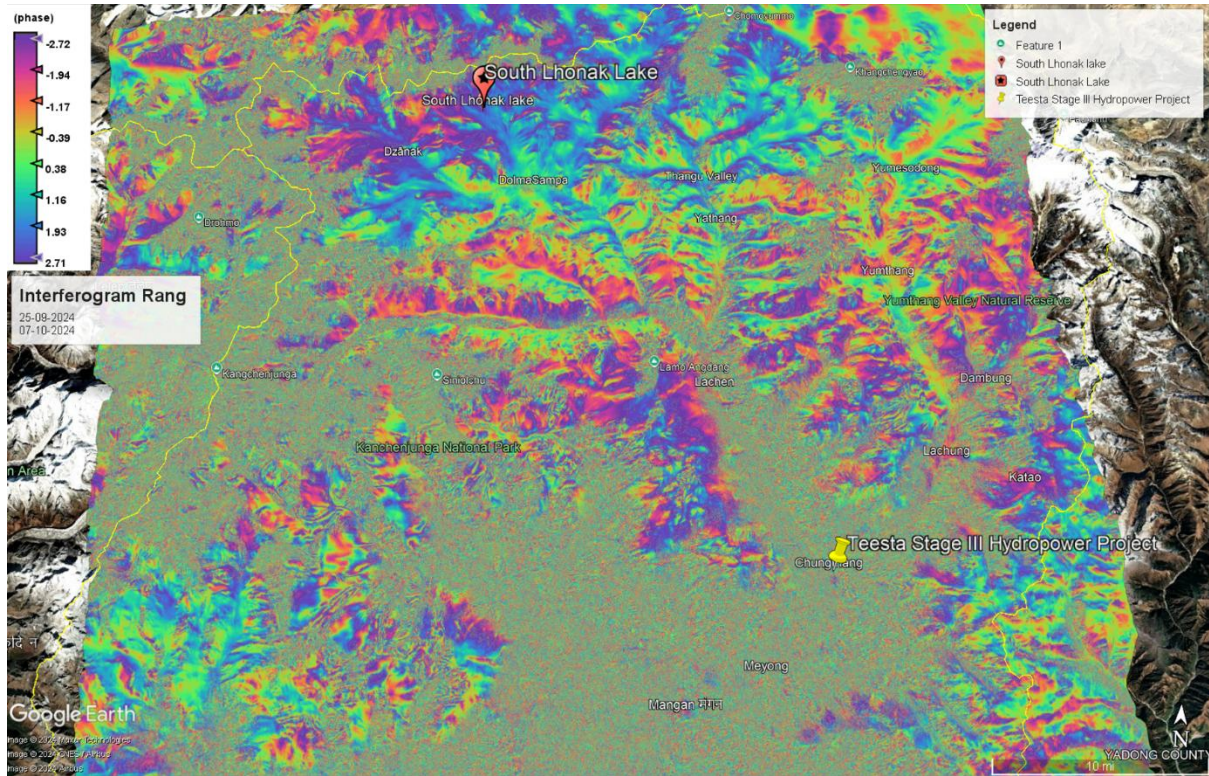


Figure 17: Processed Unwrapped Interferogram, (Projected on Google Earth Pro)

Interpreting the Fringes:

- **Closer-Spaced Fringes:** Indicate steeper slopes (for topography) or rapid displacement (for deformation).
- **Wider-Spaced Fringes:** Represent gentler slopes or slower displacement.
- **Color Coding:** Colors in an interferogram represent the degree of phase difference. The color sequence usually repeats in a cyclic manner to indicate phase wrapping.
- **Phase Wraps:** The phase values are cyclical, ranging from $-\pi$ to $+\pi$. The phase values are cyclical, ranging from $-\pi$ to $+\pi$.

5.2 Displacement Map

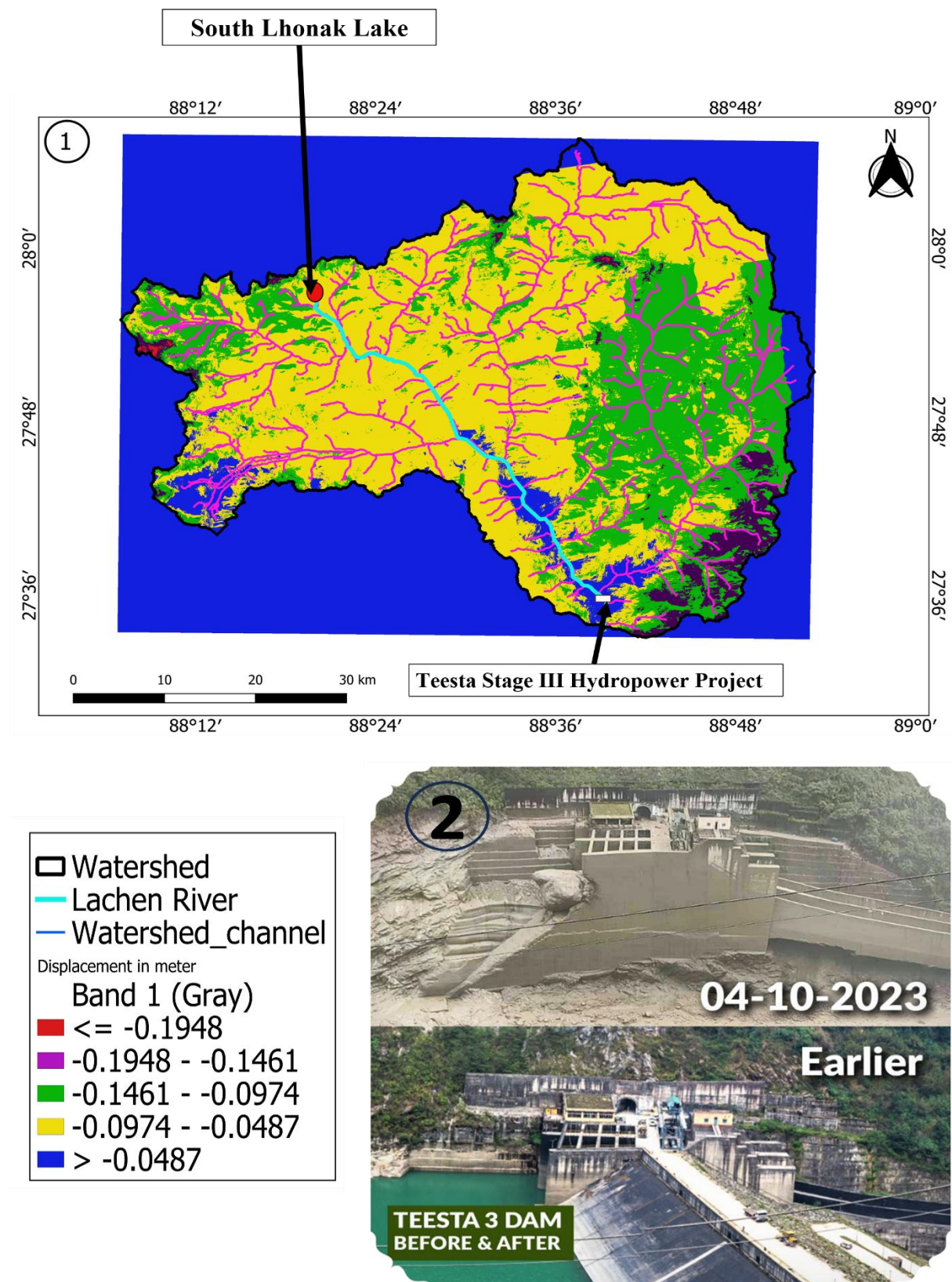


Figure 18:(1) Image generated from SNAP which showing displacement ranging from -0.0487 m to -0.01948 m in water shed area, (2) Teesta stage 3 Dam before event and after dam breach, source: SANDRP web, 2018.

6. Chapter

6.1 Future Scope

1. Early Warning System: Provide actionable data to prevent dam failures by identifying potential risks
2. Environmental Monitoring: Evaluate external factors like subsidence, uplift, or landslides near reservoirs.
3. To monitor sediment Erosion and deposition along the longitudinal slope of river bank.
4. InSAR-Based Time-Series Analysis deformation of Dam area and upstream area.

7. REFERENCES

- F. Gama, F., Mura, J. C., R. Paradella, W., & G. de Oliveira, C. (2020). Deformations prior to the Brumadinho dam collapse revealed by Sentinel-1 InSAR data using SBAS and PSI techniques. *Remote sensing*, 12(21), 3664. <https://doi.org/10.3390/rs12213664> .
- Dwitya, R., Pratomio, A. H., Cahyadi, T. A., Nugroho, A. R. B., Utomo, D. P., & Sulo, C. (2024, May). Slope Stability Monitoring of Hydroelectric Dam and Upstream Watershed Areas Utilizing Satellite Interferometric Synthetic Aperture Radar (InSAR). In *IOP Conference Series: Earth and Environmental Science* (Vol. 1339, No. 1, p. 012037). IOP Publishing. <https://doi.org/10.1088/1755-1315/1339/1/012037> .
- Antonielli, B., Caporossi, P., Mazzanti, P., Moretto, S., & Rocca, A. (2018, July). InSAR & photomonitoringtm for dams and reservoir slopes health & safety monitoring. In *Proceedings of the Twenty-Sixth International Congress on Large Dams/Vingt-Sixième Congrès International des Grands Barrages, Vienna, Austria* (pp. 4-6). DOI 10.3217/978-3-85125-620-8-227.
- Wang, T., Perissin, D., Rocca, F., & Liao, M. S. (2011). Three Gorges Dam stability monitoring with time-series InSAR image analysis. *Science China Earth Sciences*, 54, 720-732, Wang, T., Perissin, D., Rocca, F., & Liao, M. S. (2011). Three Gorges Dam stability monitoring with time-series InSAR image analysis. *Science China Earth Sciences*, 54, 720-732.
- F. Gama, F., Mura, J. C., R. Paradella, W., & G. de Oliveira, C. (2020). Deformations prior to the Brumadinho dam collapse revealed by Sentinel-1 InSAR data using SBAS and PSI techniques. *Remote sensing*, 12(21), 3664; <https://doi.org/10.3390/rs12213664>.
- Rana, N. M., Delaney, K. B., Evans, S. G., Deane, E., Small, A., Adria, D. A., ... & Take, W. A. (2024). Application of Sentinel-1 InSAR to monitor tailings dams and predict geotechnical instability: practical considerations based on case study insights. *Bulletin of Engineering Geology and the Environment*, 83(5), 204, <https://doi.org/10.1007/s10064-024-03680-3> .
- Goff, C., Ainscoe, E., Liu, Y., & Roca, M. (2021). Satellite data for dam safety monitoring. *Dams and Reservoirs*, 31(3), 90-100. <https://doi.org/10.1680/jdare.21.00021> .

- Scaioni, M., Marsella, M., Crosetto, M., Tornatore, V., & Wang, J. (2018). Geodetic and remote-sensing sensors for dam deformation monitoring. *Sensors*, 18(11), 3682. <https://doi.org/10.3390/s18113682> .
- Pipitone, C., Maltese, A., Dardanelli, G., Lo Brutto, M., & La Loggia, G. (2018). Monitoring water surface and level of a reservoir using different remote sensing approaches and comparison with dam displacements evaluated via GNSS. *Remote Sensing*, 10(1), 71. DOI [10.3390/rs10010071](https://doi.org/10.3390/rs10010071).
- SANDRP web (South Asia Network on Dams, Rivers and People), 2018 <https://sandrp.in/wp-content/uploads/2018/03/teesta-150411.jpg> (accessed on 22/11/2024).
- SANDRP web (South Asia Network on Dams, Rivers and People), 2018 <https://sandrp.in/2023/10/04/glacial-lake-flood-destroys-teesta-3-dam-in-sikkim-brings-wide-spread-destruction/> (accessed on 26/11/2024).
- ElGharbawi, T., & Tamura, M. (2015). Coseismic and postseismic deformation estimation of the 2011 Tohoku earthquake in Kanto Region, Japan, using InSAR time series analysis and GPS. *Remote Sensing of Environment*, 168, 374-387. <https://doi.org/10.1016/j.rse.2015.07.016>
- Pezzo, G., Palano, M., Beccaro, L., Tolomei, C., Albano, M., Atzori, S., & Chiarabba, C. (2023). Coupling flank collapse and magma dynamics on stratovolcanoes: the Mt. Etna example from InSAR and GNSS observations. *Remote Sensing*, 15(3), 847. <https://doi.org/10.3390/rs15030847> .
- Sinha, K., Sharma, P., Sharma, A., Singh, K., & Hassan, M. (2024). Analysis of Land Subsidence in Joshimath Township using GIS and Remote Sensing. *Journal of Mining and Environment*, 15(3), 817-843. <https://doi.org/10.22044/jme.2024.13776.2556>.
- Renalt Capes Source web (https://www.researchgate.net/figure/llustration-of-ascending-and-descending-satellite-orbits_fig1_310799583).
- Alaska Satellite Facility (ASF), NASA-Indian Space Research Organization (ISRO) Synthetic Aperture Radar workshop 2024, web <https://asf.alaska.edu/training-resources/> .

